ABSTRACT

MEASUREMENTS OF NUCLEAR RESONANCE FLUORESCENCE ON THE 1.27 Mev LEVEL OF Sn^{116}

by John M. Gonser

The 1.27 Mev level of Sn^{116} was investigated by nuclear resonance fluorescence techniques. Momenta from previous emissions were used to restore the resonance condition to a gaseous source. Weakness of the source prevented accurate determination of the mean life of the 1.27 Mev state which was found to be less than $0.84 \pm 0.7 \times 10^{-12}$ seconds.

MEASUREMENTS OF NUCLEAR RESONANCE FLUORESCENCE ON THE 1.27 Mev LEVEL OF Sn^{116}

by

John M. Gonser

A THESIS

Submitted to
Michigan State University
in partial fulfillment of the requirements
for the degree of

MASTER OF SCIENCE

Department of Physics

1964

To Marilyn

ACKNOWLEDGMENT

The author wishes to express his gratitude to Dr. W. H. Kelly for his guidance throughout this endeavor, and to Dr. G. B. Beard for his added guidance during the experimental phase, and to the Michigan State University Department of Physics and the U.S. Air Force Office of Scientific Research for their financial support. The author wishes also to thank Mr. William Dunbar of the University of Michigan Phoenix Reactor staff, and to Mr. D. G. Parker and Mr. M. Mallory for their assistance.

TABLE OF CONTENTS

		Page
I.	INTRODUCTION	1
	Definition	1
	Historical Background	1
II.	EXPERIMENTAL CONSIDERATIONS	6
	Sample Preparation	6
	Apparatus	10
III.	CALCULATIONS	16
	Cross-Section for Resonance Fluorescence	16
	Doppler Line Shape	18
IV.	RESULTS	26
	Data Analysis	26
	Conclusions	30
	BIBLIOGRAPHY	31

INDEX OF FIGURES

Figure		Page
1	Decay Scheme for 54 min. In^{116}	5
2	Gamma-Ray Spectrum of Sn^{116}	8
3	Block Diagram of Experimental Apparatus	9
4	Scattering Apparatus	13
5	Oven for Source	14
6	Plot of Counts Detected due to Test Source on Ring	15
7	Emission of First Gamma	20
8	Emission of Second Gamma	22
9	Line Shape of 1.27 Mev Level in Sn^{116}	25
10	Composite Plot of One Day's Data	27

I. INTRODUCTION

Definition

Nuclear resonance fluorescence is the name given to a particular class of gamma-ray scattering phenomena. This class is distinguished by resonance in its interactions, as opposed to those classes in whose interactions the quality of resonance is absent. Resonance can occur in a target nucleus which has an excited state whose preferred mode of de-excitation to the ground state is a single gamma-ray transition.

The primary body of information obtainable from nuclear resonance fluorescence is contained in the relative intensity of the resonance line in a scattering or an absorption experiment. From this intensity the average cross-section for resonance fluorescence may be found. This average cross-section is related to transition probability of the de-excitation gamma-ray, which, in turn, is related to the level width of the excited state of the nucleus. Once the level width is known, the lifetime of the excited state is found through use of the uncertainty relationship.

Historical Background

The existance of resonance fluorescence phenomena in atomic transitions was known and verified experimentally before a single successful nuclear resonance fluorescence experiment was carried out. In 1929 Kuhn [1]* suggested the possibility of the nuclear analogue to atomic resonance fluorescence and performed an unsuccessful experiment in an attempt to

---

* The numbers in square brackets refer to references listed in the Bibliography.

detect this effect. The next few years brought forth other similarly unsuccessful attempts [2], [3] in which the researchers were relying on the natural width of the emission and absorption lines to produce the conditions for resonance fluorescence. Actually, the occurrence of resonance fluorescence depends strongly on the Doppler shifts in the emitted gamma-rays due to previous emissions as well as the emission and absorption in question.

This is due to the fact that a photon emitted by a nucleus gives up some of its energy to the nucleus in the form of recoil energy. This Doppler energy loss is large compared to the natural width of the emission and absorption lines in the nuclear case. Thus, the possibility of observing nuclear resonance fluorescence through overlap of the absorption and emission lines is slight. In the atomic case this is not so; the natural line widths are large compared to the recoil energy losses, and atomic resonance will occur by natural overlap of the absorption and emission lines. Therefore, success in observing nuclear resonance lies in restoration of the Doppler energy losses to the gamma-ray so that the emission and absorption lines will overlap.

The effect of the Doppler shifts due to nuclear recoil may be studied by conservation considerations. Such a study is given below. Non-relativistic velocities are assumed throughout.

Momentum conservation requires that when a nucleus emits a particle the nucleus recoil with a momentum equal and opposite to the momentum of the particle. The gamma-ray, then, yields some energy to the nucleus in

the form of recoil energy. The amount of energy lost in this manner may be found through the conservation laws. If the assumption of a freely-recoiling nucleus is made and if the emitted particle is a gamma-ray, then conservation of momentum states:

$$Mv = E_\gamma/c,$$

where E = energy of the gamma-ray,

M = mass of the nucleus,

and v = velocity of the nucleus due to recoil.

The energy conservation statement for this reaction is:

$$\frac{1}{2} Mv^2 + E_\gamma = E_o,$$

where E_o is the transition energy.

The gamma-ray energy differs from the transition energy by an amount $Mv^2/2$, or

$$E_\gamma = E_o' - \frac{E_\gamma^2}{2Mc^2}$$

As an example, the 1.27 Mev gamma-ray transition in Sn^{116} results in a Doppler shift in the energy of 16 ev, assuming the Sn^{116} nucleus recoils freely. Thus, the energy left to the gamma-ray is 1.27 Mev minus 16 ev. On the basis of results of Coulomb excitation experiments [14], the natural line width is of the order of 10^{-3} ev. This means that the Doppler shift is several orders of magnitude larger than the expected line width, and so, overlap of the emission and absorption lines is prevented.

If the gamma-ray is now allowed to impinge on a nucleus of mass M that can recoil freely, then another amount of energy

$$\frac{E'_\gamma{}^2}{2Mc^2}$$

is lost to this nucleus in recoil. Now, since

$$\frac{E'_\gamma{}^2}{2Mc^2} \approx \frac{E_\gamma{}^2}{2Mc^2}$$

the total amount of energy lost by the gamma-ray is approximately

$$\frac{E_\gamma{}^2}{Mc^2} = \Delta E$$

Thus, in order for resonance of this gamma-ray with the level E_o to exist, energy of the magnitude ΔE must be restored to the gamma-ray by some outside source.

The first successful observation of the resonance fluorescence phenomenon was made by Moon [4] in 1951. Moon concentrated on the restoration of the resonance condition by external means. For this purpose, an air-driven ultra-centrifuge was utilized, and speeds up to 7×10^4 cm/sec at the periphery were obtained, which were sufficient to restore the resonance condition to Hg^{198}.

A later effort by Malmfors [5] used thermal agitation to restore the resonance condition in the same isotope. In this case a source of Au^{198} was heated in an oven in much the same arrangement as in the present consideration.

More recent investigations, [6], [7], as well as the present one, have utilized the Doppler shifts due to previous radiation in a gaseous source to bring about correct conditions for resonance fluorescence.

DECAY SCHEME FOR 54 MIN. In^{116} [8]

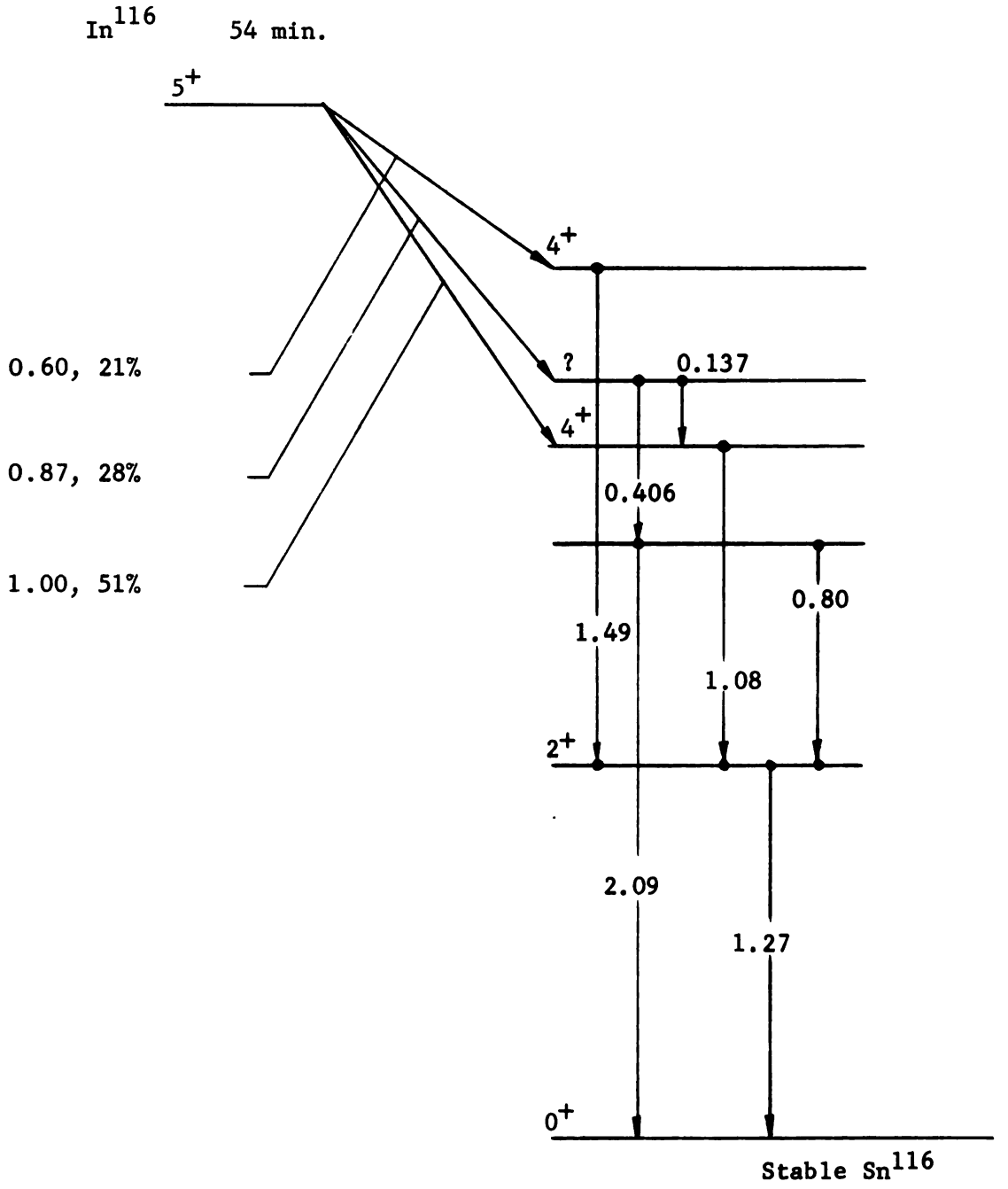

FIGURE 1

II. EXPERIMENTAL CONSIDERATIONS

Sample Preparation

The decay scheme for Sn^{116} is given in Figure 1. From this decay scheme it is seen that the 1.27 Mev level decays directly to the ground state by a gamma-ray transition, and that it has but one mode of de-excitation. The necessity of using a level which decays directly to the ground state is due to the use of a ground state nucleus as a target. The fact that there is only one mode of de-excitation, a gamma-ray, lends to ease in analysis, as will be seen in a later section (see Section III).

The decay scheme in Figure 1 shows a 1.49 Mev transition following an 0.60 Mev beta. At this point, it would appear that the Doppler shift in the energy of the 1.27 Mev gamma-ray due to this beta-gamma cascade could restore the resonance condition to the 1.27 Mev gamma-ray. Consideration of the other decay modes leading to the 1.27 Mev level suggest that they may aid in the restoration of the resonance condition. This is investigated further in a later section (see Section III). Therefore, it was decided to utilize this Doppler broadening of the 1.27 Mev level due to these previous emissions to restore the momentum lost to the 1.27 Mev gamma-ray through recoil.

Promotion of the Doppler broadening is attained by lengthening the mean free path; i.e., making the source gaseous. This also serves to approximate more nearly the case of freely-recoiling nuclei. The source was made gaseous by combining it before irradiation (In^{116}) with chlorine

to form $InCl_3$. A small amount of this was dissolved in concentrated HCL and placed in one section of a two-section quartz ampoule. The sample was then frozen and evacuated, driving off excess water.

After this operation, the sample, while still in the vacuum system, was heated slightly to drive off any remaining water. Then the sample was evacuated further and distilled over into the second section of the ampoule, whose volume was approximately 5 cm^3. This section was then sealed off and removed from the rest of the system.

The sample was irradiated in the Ford Reactor of the Phoenix Laboratory, University of Michigan in Ann Arbor, Michigan. Irradiation times upwards of two hours were used at a flux of 5×10^{12} cm^{-2} sec^{-1}. From two to three hours elapsed between the removal of the sample from the reactor and the beginning of the first experimental run. At this time, the strength of the source was about one millicurie, for a 5×10^{-4} gm. sample.

The gamma-ray spectrum for a typical sample is shown in Figure 2. This spectrum was taken from the data acquired by the monitor side of the apparatus shown in Figure 3. In order to obtain these data, a 1.5 inch diameter x 1 inch high NaI(Tl) scintillation crystal with photomultiplier apparatus was placed 190 cm from the source. Because a spectrum which would be free from scattering or attenuation effects was desired, the scintillation crystal was placed so it had a relatively unimpeded view of the source. These data were used to monitor the strength of the source throughout the course of the experiment, and such data were taken concurrently with nearly every run.

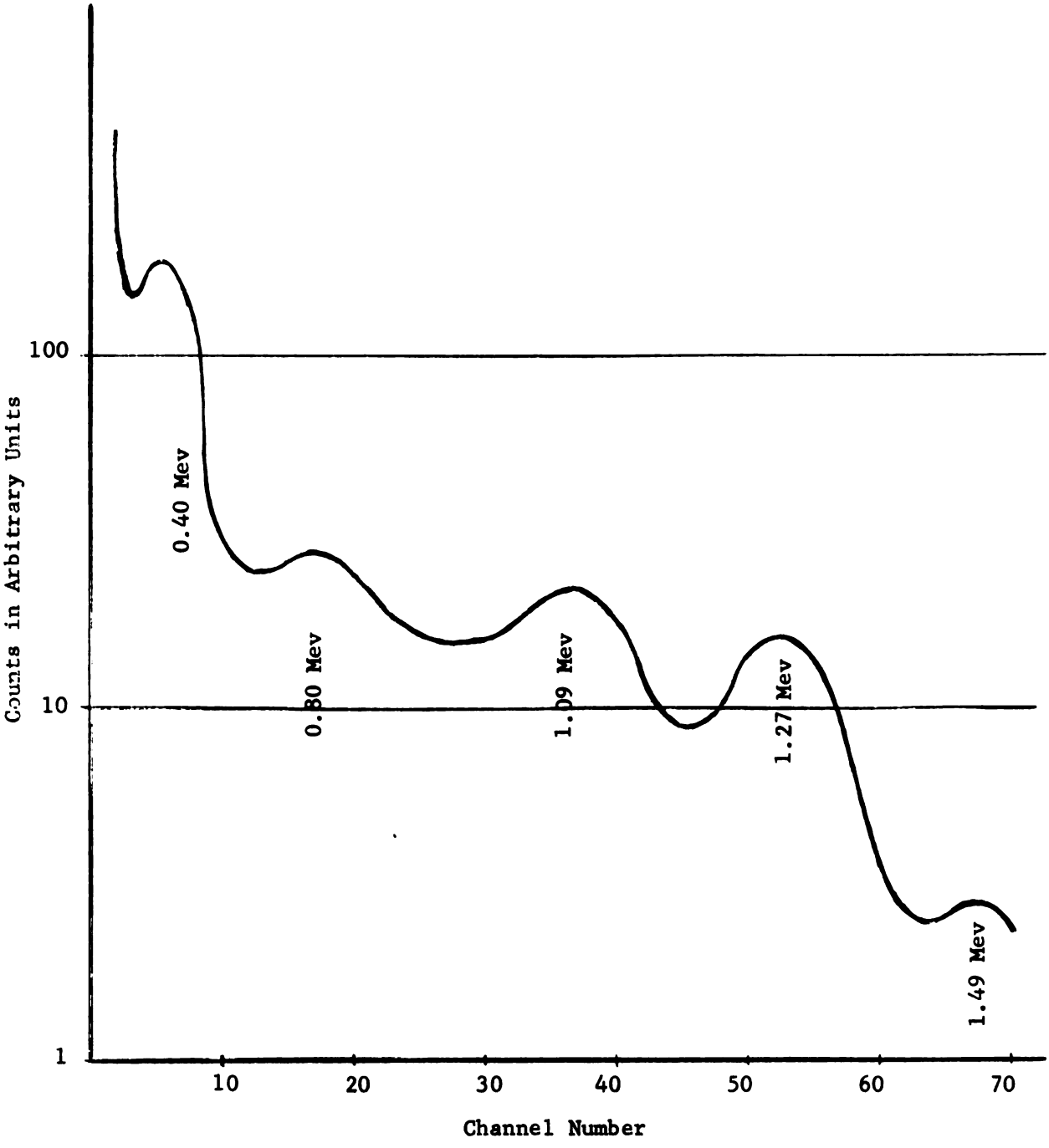

GAMMA-RAY SPECTRUM
OF Sn^{116}

FIGURE 2

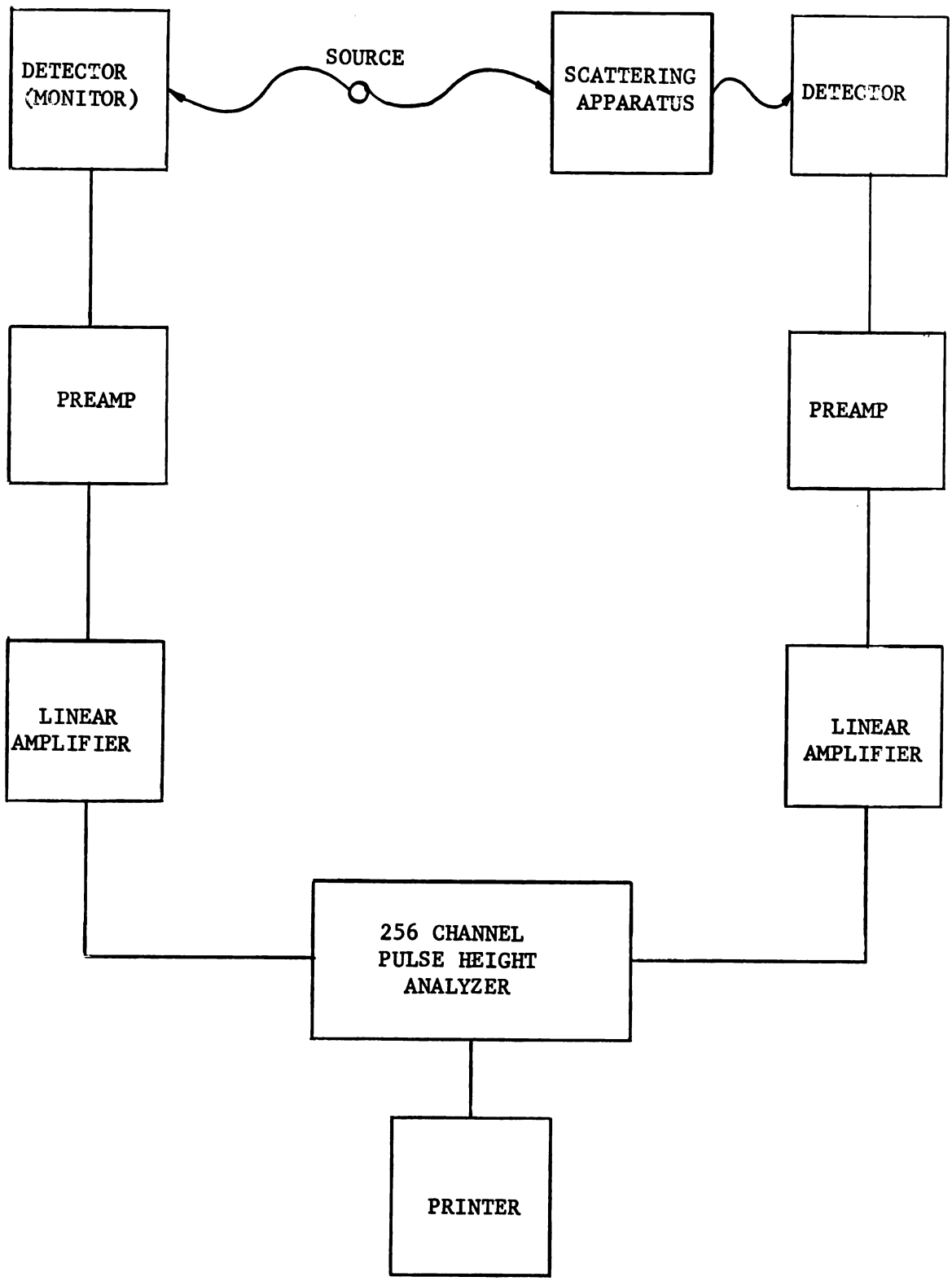

BLOCK DIAGRAM OF
EXPERIMENTAL APPARATUS

FIGURE 3

Apparatus

A method of measuring the average cross-section for resonant scattering is desired. For this measurement a source, scatterer, and detector are needed, along with suitable shielding to prevent detection of unscattered radiation. The scattering apparatus used in the present consideration is shown in Figure 4.

The scattering ring for resonance fluorescence was made of tin, and was arranged so it could be replaced quickly by a non-resonant scattering ring of like dimensions. This was to allow a comparison between the resonant and non-resonant components. The material chosen for the non-resonant scattering ring was cadmium, while the resonant scattering ring was tin. The choice of cadmium was made because of the nearness of the atomic number of cadmium to that of tin. This allowed approximately equal attenuation due to electronic absorption effects in the two scattering rings [18]. The oven arrangement shown in Figure 5 allowed wide variations in the source temperature so it could be made gaseous or solid at will. The oven temperature was commonly held at 750°C, to assure a gaseous source [8]. The tin-lead graded absorber at the crystal was used to attenuate the large number of Compton scattered photons detected by the crystal.

Some of the 1.27 Mev gamma-rays originating at the source will impinge on the scattering ring. Some of these, depending on the cross-section for nuclear resonance fluorescence, can excite Sn^{116} nuclei in the scatterer to their 1.27 Mev state and be re-radiated. Some of these re-radiated

gamma-rays can be detected by the crystal and stored as counts by the associated electronic apparatus. The crystal was prevented from detecting unscattered radiation by the tungsten-lead shield shown in Figure 4. A block diagram of the electronic system used is shown in Figure 3.

In order to relate correctly the number of events detected by the crystal to the number occurring at the source (hence, to the cross-section σ_{av}), the effects of the geometry of the system must be considered. This means that the solid angles between the source and scattering rings, and between the scattering ring and the crystal must be used in the calculations of σ_{av}.

The solid angle subtended by the crystal at the scattering ring is not easily calculated and an empirical method was employed. The approach used here was measuring the relative source strength of a known source as detected by the crystal. The source used was the 1.33 Mev gamma level in Co^{60} because of the nearness of this level to that level under investigation, 1.27 Mev. The source was moved in 1/4" intervals vertically on the inside of the scattering ring, and data were taken at each point. A graph of these data is shown in Figure 6.

The mean value of these data, when compared to the source strength, provides a measure of the probability that an event in the 1.3 Mev range occurring on the scattering ring will be detected by the crystal. This probability may be regarded as a composite factor consisting of the solid angle in question, the attenuation due to the Pb-Sn graded absorber, the crystal efficiency, and the photofraction. Thus,

$$\Omega_D \, A\eta_p = \frac{\text{Number of counts detected}}{\text{Number of disintegrations occurring at the ring}}$$

where Ω_D = fractional solid angle subtended by the detector at the scatterer,

A = attenuation due to the Pb-Sn absorber,

η = crystal efficiency,

p = photofraction.

This composite factor is used in later calculations.

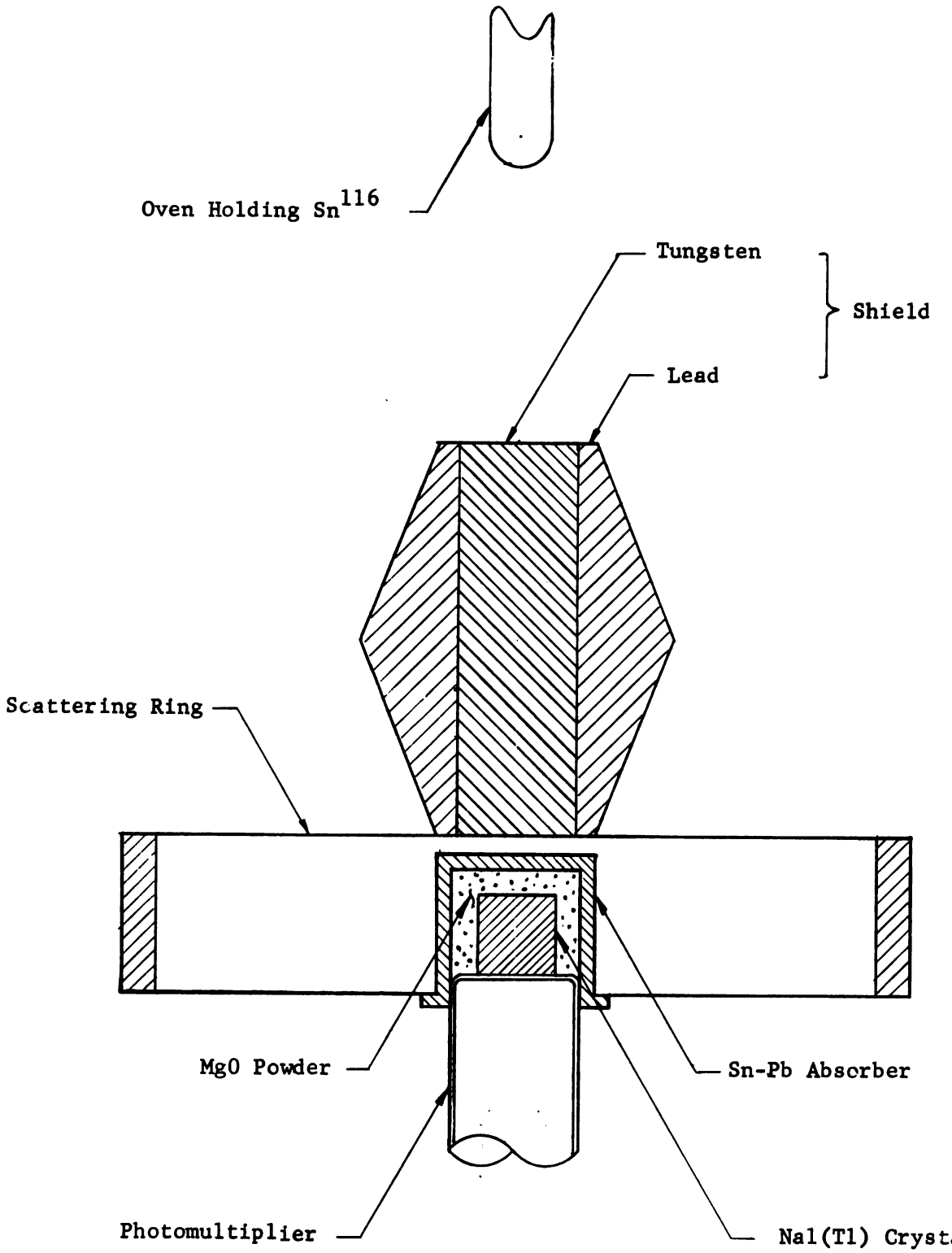

SCATTERING APPARATUS

FIGURE 4

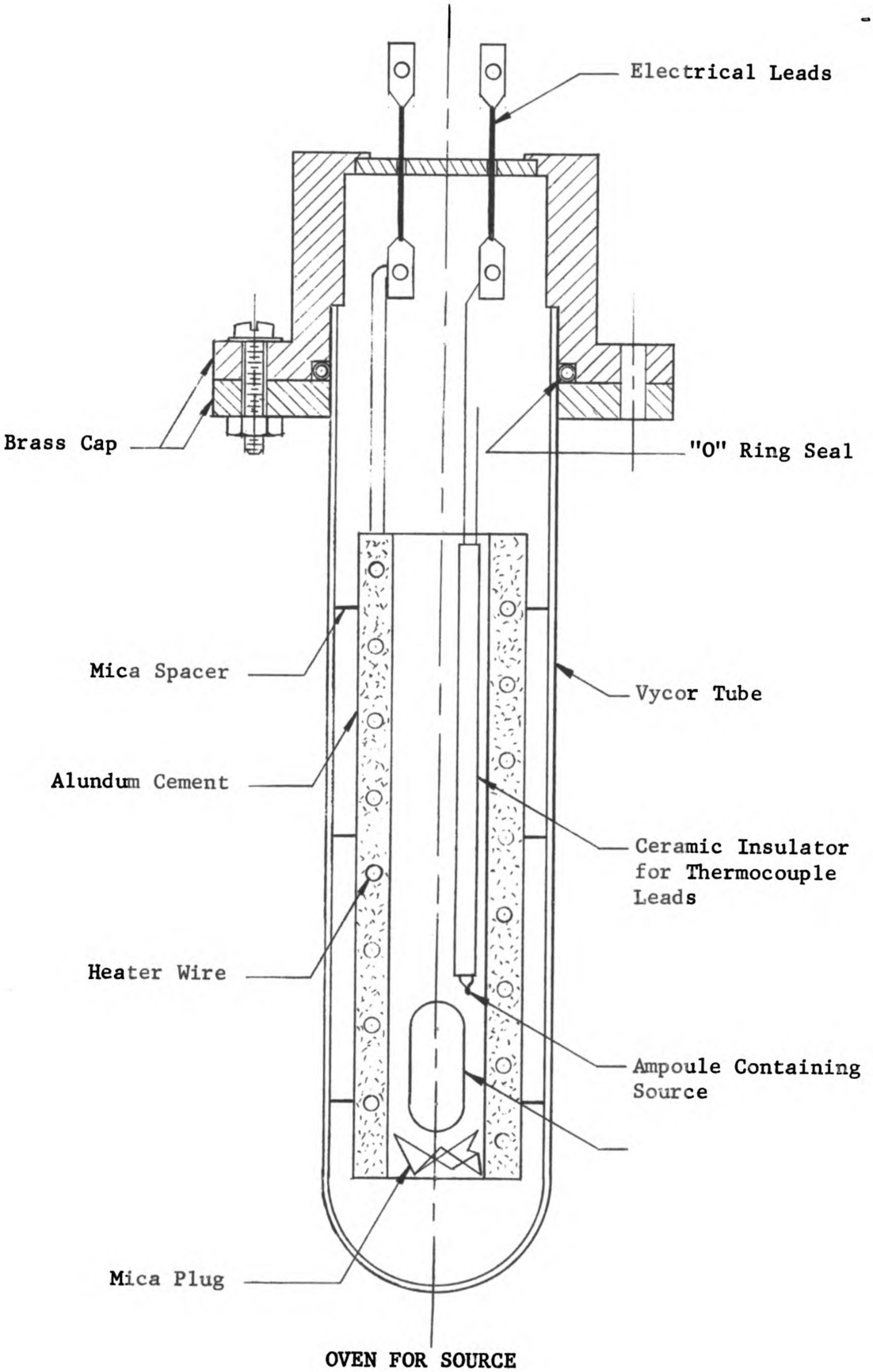
Electrical Leads
Brass Cap
"O" Ring Seal
Mica Spacer
Vycor Tube
Alundum Cement
Ceramic Insulator for Thermocouple Leads
Heater Wire
Ampoule Containing Source
Mica Plug
OVEN FOR SOURCE

FIGURE 5

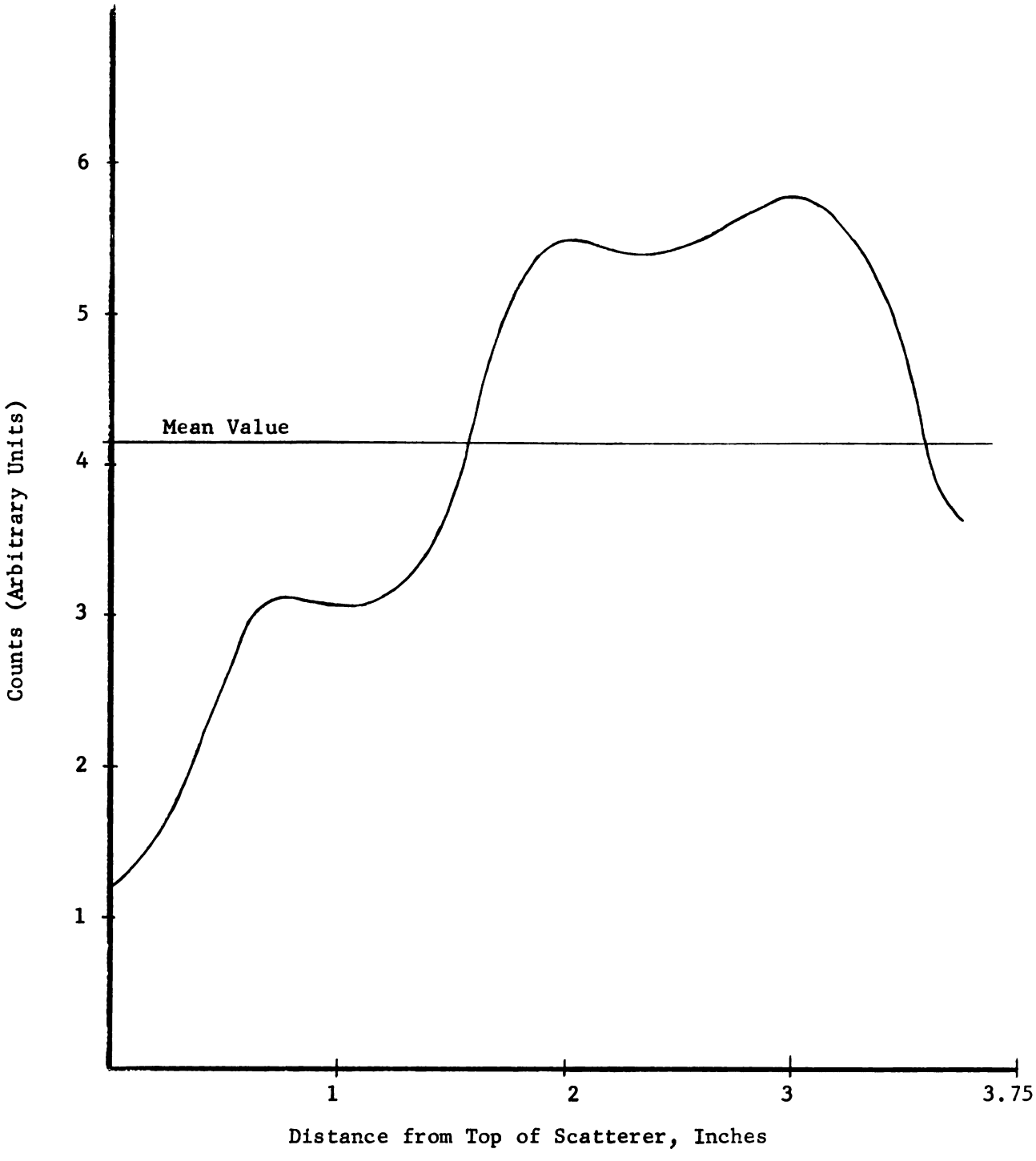

PLOT OF COUNTS DETECTED DUE TO
TEST SOURCE ON RING

FIGURE 6

III. CALCULATIONS

Cross Section for Resonance Fluorescence

The cross section for resonance fluorescence is given by an expression of the Lorentz shape [9], [10]

$$\sigma(E) = \frac{2J_1 + 1}{2J_o + 1} \frac{\lambda^2 \Gamma_o \Gamma_i}{8\pi\left[(E - E_\gamma)^2 + (\Gamma/2)^2\right]} \tag{1}$$

where σ = cross section for resonance fluorescence,

J_1, J_o = spins of the excited and ground levels, respectively,

λ = wavelength of the resonance photon,

Γ_o, Γ_i = partial level widths for direct transition to ground, and for transition through the mode in question, respectively,

E = energy of the incident photon,

E_γ = E at resonance,

and Γ = total natural width of the excited level.

In the present case the internal conversion may be neglected [11], so the major mode of decay from the 1.27 Mev level will be through photons which will be available for resonance fluorescence. Therefore, expression (1) becomes

$$\sigma(E) = \frac{2J_1 + 1}{2J_o + 1} \frac{\lambda^2 \Gamma^2}{8\pi\left[(E - E_\gamma)^2 + (\Gamma/2)^2\right]} \tag{2}$$

In practice, the cross-section is determined by the number of gamma-rays resonantly scattered from a scatterer of finite dimensions. Analysis of such a situation is made easier for the case where the natural width Γ

is much smaller than the thernal Doppler width Δ, where

$$\Delta = E\left(\frac{2k\ T}{Mc^2}\right)^{1/2}$$

Here k = Boltzmann's constant,

and T = absolute temperature.

This limitation of Γ, however, is good for most gamma lines. As an example, for the 1.27 Mev level of Sn^{116} the thermal Doppler width is of the order of 1 ev, while the natural width is of the order of 10^{-3} ev. In these cases, the cross-section has the Doppler form [6]

$$\sigma_D(E) = \left(\frac{2J_1 + 1}{2J_o + 1}\right) \frac{\Gamma\ \lambda^2}{4\sqrt{\pi}\ \Delta}\ e\ \left\{-(E - E_\gamma)^2/\Delta^2\right\}$$

This form for $\sigma_D(E)$ is normally used to compute results in a self-absorption experiment. However, in the present case the sources were too weak to permit such an experiment to be performed.

Equation (2) represents a sharply-peaked function of energy. The average value of the cross-section, σ_{av}, is the measurable quantity. To obtain this

$$\sigma_{av} = \frac{\int \sigma(E)\ N(E)\ dE}{\int N(E)\ dE}$$

where the integrals are taken over the incident spectrum. As mentioned above, $\sigma(E)$ is a sharply-peaked function, and so N(E), being slowly varying in the region of resonance, may be regarded as constant at $E = E_{res}$, the resonant energy. This energy, E_{res}, is the energy at which $\sigma(E)$ reaches its maximum value. Hence,

$$\sigma_{av} = \frac{N(E_{res}) \int \sigma(E)\, dE}{N}. \tag{3}$$

If the de-excitation mode is restricted as previously stated, the integral in equation (3) is

$$\int \sigma(E)\, dE = \frac{2J_1 + 1}{2J_o + 1} \frac{1}{8\pi} \int \frac{\lambda^2 \Gamma^2}{\left[(E - E_{res})^2 + (\Gamma/2)^2\right]} dE,$$

where the integration is to be carried out over the incident spectrum. This has been done [17] with the result

$$\int \sigma(E)\, dE = \frac{2J_1 + 1}{2J_o + 1} \left(\frac{\lambda_o}{2}\right)^2 \Gamma$$

Substitution into equation (3) gives

$$\sigma_{av} = \frac{N(E_{res})}{N} \frac{2J_1 + 1}{2J_o + 1} \left(\frac{\lambda_o}{2}\right)^2 \Gamma \tag{4}$$

Heisenberg's principle states

$\tau\Gamma \sim \hbar$, where τ is the mean lifetime of the state so that substitution into equation (4) for Γ will give

$$\sigma_{av} = \frac{N(E_{res})}{N} \frac{2J_1 + 1}{2J_o + 1} \left(\frac{\lambda_o}{2}\right)^2 \frac{\hbar}{\tau} \tag{5}$$

Once σ_{av} is obtained from the experiment, the calculation of $N(E_{res})/N$ must be made in order to use equation (4) to relate σ_{av} to τ. The value of $N(E_{res})/N$ is estimated through knowledge of the line shape of the incoming radiation and is explored in the next section.

Doppler Line Shape

The value of $N(E_{res})/N$ can be estimated from information about the nature of the recoil process. This ratio represents the shape of the emission line and depends on Doppler shifts due to previous radiations

and thermal broadening. In order to obtain a numerical value for this ratio the various modes of decay to the 1.27 Mev level must be investigated as to their effect on the line shape of that level. The assumption is made that the nuclei recoil freely. Also, for simplicity, it is assumed the molecules remain intact upon emission of a particle.

Figure 1 shows there are a total of four cascades which lead to the 1.27 Mev level: two of these involve one beta and one gamma transition preceeding the 1.27 Mev level, and two involve one beta and two gamma transitions preceeding the 1.27 Mev level. These are the 1.00 Mev beta - 1.08 Mev gamma, 0.60 Mev beta - 1.49 Mev gamma, 0.87 Mev beta - 0.137 Mev gamma - 1.08 Mev gamma, and the 0.37 Mev beta - 0.406 Mev gamma - 0.80 Mev gamma cascades, each of which is followed by the 1.27 Mev gamma transition. The remaining cascades are ignored because they do not lead to the 1.27 Mev level.

The effect of these cascades on the gamma line shape may be found (see Section I) by energy and momentum considerations. Such an analysis is carried out below, for the case where the preceeding radiation is a beta-gamma-gamma cascade. Similar procedures may be used for analysis of other cascades.

If a nucleus of mass M emits a beta particle of momentum P_β, the nucleus will recoil with a velocity v_1. The kinetic energy of the nucleus, assumed initially to be at rest, is then

$$T = \frac{1}{2} M v_1^2$$

Conservation of momentum requires that

$$P_\beta = Mv_1.$$

If the nucleus now emits a gamma-ray, the energy requirement is for this emission

$$E_2 + \frac{1}{2} Mv_1^2 = E_{\gamma 2} + \frac{1}{2} Mv_2^2,$$

where E_2 = transition energy of the gamma emission,

$E_{\gamma 2}$ = energy of the gamma-ray,

v_2 = velocity of the nucleus after emission of the gamma-ray.

From Figure 7, the momenta are resolved into components along the direction of the gamma and perpendicular to it. For the components parallel to γ_2,

$$E_{\gamma 2}/c - Mv_1 \cos \theta = Mv_2 \cos \phi$$

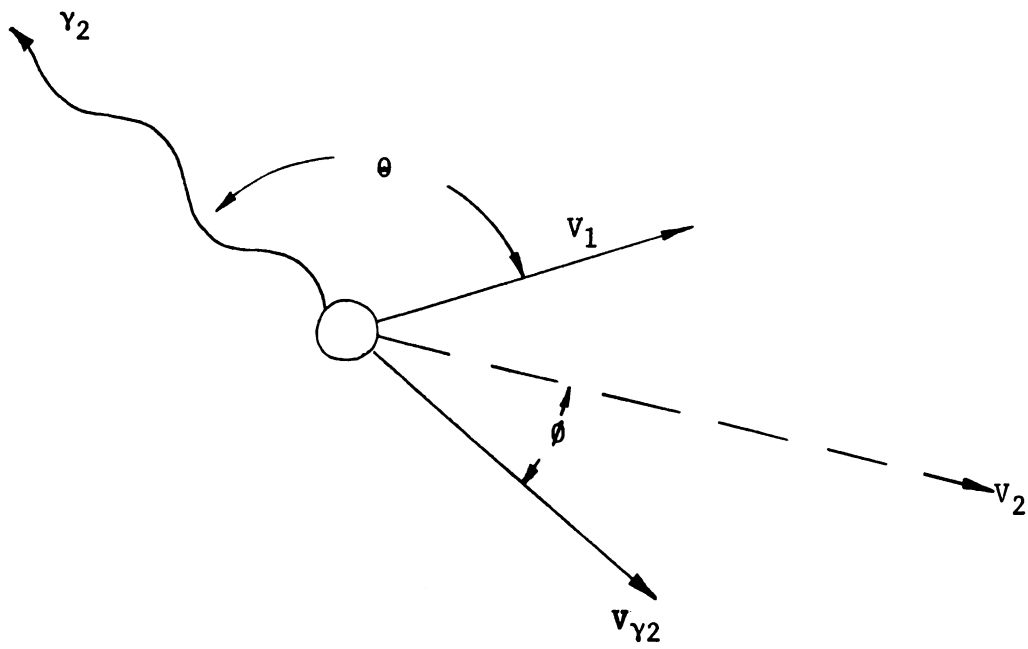

Figure 7

For the components perpendicular to γ_2,

$$Mv_1 \sin \theta = Mv_2 \sin \phi.$$

Elimination of ϕ between the expressions for the components of momentum leads to the equation

$$\frac{E_{\gamma 2}^2}{2Mc^2} + \frac{1}{2} Mv_1^2 - \frac{E_\gamma^2}{Mc} Mv_1 \cos \theta = \frac{1}{2} Mv_2^2.$$

This expression, in conjunction with the energy equation for this gamma emission, may be used to eliminate v_2. The resulting expression will give E_2 as a function of $E_{\gamma 2}$, v_1, and θ. This expression is

$$E_2 = E_{\gamma 2} + \frac{E_{\gamma 2}^2}{2Mc^2} - \frac{E_\gamma^2}{Mc} Mv_1 \cos \theta.$$

Since the end result of this analysis is to show the effect of these two emissions on the second gamma-ray, it will be well to introduce this emission. Calling this second gamma-ray γ_3, to identify it as the third emission, a similar procedure to that above leads to the expression

$$E_3 = E_{\gamma 3} + \frac{E^2_{\gamma 3}}{2Mc^2} - \frac{E_{\gamma 2}}{Mc} Mv_2 \cos \psi,$$

where E_3 = transition energy of the γ_3 level,

E = energy of γ_3

and ψ = angle between v_2 and γ_3. (See Figure 8)

As before, it is desirable to eliminate v_2, since it is not a determined quantity. This may be done through the momentum components for the emission of γ_2, which suggest

$$Mv_2 = (P^2_{\gamma 2} + P^2_\beta - 2P_{\gamma 2} P_\beta \cos \theta)^{1/2}$$

where $P_{\gamma 2} = \frac{E_{\gamma 2}}{c}$ = momentum of γ_2,

and $P_\beta = Mv_1$ = momentum of β.

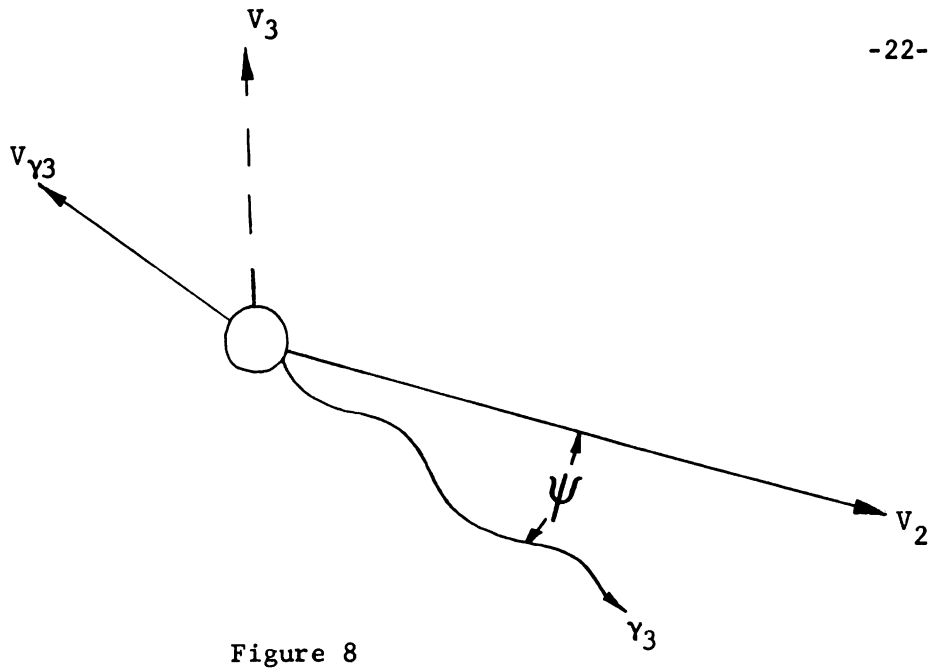

Figure 8

Substitution for Mv_2 in the expression for E_3 yields

$$E_3 = E_{\gamma 3} + \frac{E^2_{\gamma 3}}{2Mc^2} - \frac{E_{\gamma 3}}{Mc}\left[P^2_{\gamma 2} + P^2_{\beta} - 2P_{\beta} P_{\gamma 2} \cos\theta\right]^{1/2} \cos\psi.$$

This is the desired result which shows the Doppler shift in γ_3 due to previous emissions whose momenta are P_{β} and $P_{\gamma 2}$.

The preceeding development may be utilized to yield the Doppler broadening of γ_3 with the approximation suggested in Section I; that is,

$$\frac{E^2_{\gamma 3}}{Mc^2} \approx \frac{E^2_3}{Mc^2}$$

With this, then, the energy of the γ_3 photon may be written:

$$E_{\gamma 3} = E_3 - \frac{E^2_3}{2Mc^2} - \frac{E_3}{Mc}\left[P^2_{\gamma 2} + P^2_{\beta} - 2P_{\gamma 2} P_{\beta} \cos\theta\right]^{1/2} \cos\psi.$$

The Doppler line shape of γ_3 is centered about $E_3 - \frac{E^2_3}{2Mc^2}$ and depends for its form on the third term of the right member above.

The line shape may now be estimated by graphical methods. The procedure is to calculate the energy spread due to the previous emissions leading to the energy level in question, and add these graphically to produce a plot of $N(E_{res})/N$ per electron volt interval. In the present investigation the Doppler spectra due to beta emissions were regarded as triangular, as an approximation due to the shape of the beta spectrum. This approximation results in a triangular shape for the neutrino spectrum as well. The beta and neutrino emissions were considered to be isotropic.

The contributions to the line shape due to each cascade may now be calculated. For the 1.0 Mev beta - 1.08 Mev gamma cascade, the maximum momentum which may be imparted to the nucleus by the beta and neutrino emission is 2.78 $m_o c$. This means that the maximum Doppler energy shift of the 1.27 Mev photon due to this emission is $\pm$6.95 ev. The gamma in this cascade, having an energy of 1.08 Mev, can add to cause a maximum Doppler shift of $\pm$12.25 ev.

Assuming isotropic emissions, the line shape due to one cascade consists of elemental trapezoidal segments. The major base of a segment is given by the maximum Doppler energy shift due to the particular emissions. The minor base of a segment is given by the smallest combination of these same Doppler energies. The area of the trapezoidal segment is proportional to that fraction of the total emissions leading to the 1.27 Mev level which occur in the manner being considered. Hence, the height of each segment is well defined.

The line shape of the 1. - Mev beta - 1.08 Mev gamma cascade results in a bell-shaped curve whose base is 24.5 ev wide and whose height is at 0.0472 ev^{-1}. Similar curves are found for the remaining three cascades. For the 0.60 Mev beta - 1.49 Mev gamma cascade, the width is 24.24 ev, and the height is 0.0179 ev^{-1}; for the 0.87 Mev beta - 0.137 Mev and 1.08 Mev gammas, the width is 15 ev and the height is 0.0046 ev^{-1}; for the 0.87 Mev beta - 0.41 Mev and 0.80 Mev gammas, the width is 24.26 ev, and the height is 0.0081 ev^{-1}.

The composite line shape is shown in Figure 9. The center of this line shape is located a distance from the energy at which resonance will occur. This energy, E_{res}, is equal to the level energy plus the total energy lost to that photon through recoil in the emission and absorption processes of nuclear resonance fluorescence. Hence, the expression for the line shape center-to-E_{res} distance, E', is

$$E' = \frac{E^2_{\gamma 4}}{M_1 c^2} + \frac{E^2_{\gamma 4}}{M_2 c^2},$$

where E' is the distance mentioned above,

$E_{\gamma 4}$ is the gamma-ray energy in question,

and M_1 and M_2 are the masses of the emitting and absorbing nuclei. For the proposed case, E' is found to be 11.4 ev. From Figure 9, the value for $N(E)/N$ at $E = E_{res}$ is found to be 0.004 per ev.

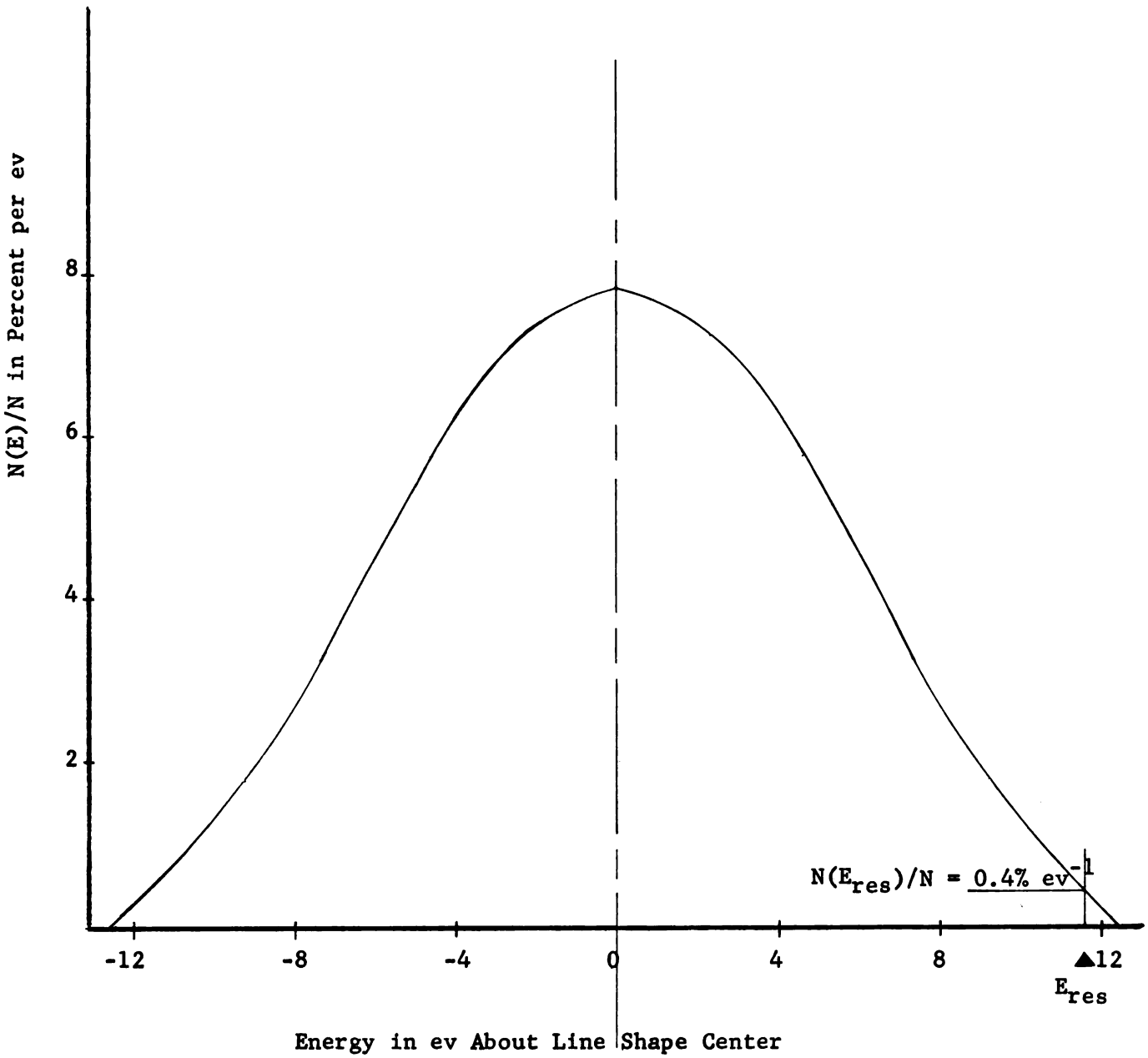

LINE SHAPE OF 1.27 Mev GAMMA IN Sn^{116}

FIGURE 9

IV. RESULTS

Data Analysis

A composite set of data is shown in Figure 10. These data are the sums of the data taken over one entire day. Figure 10 consists of three separate plots: one for resonant scattering, one for non-resonant scattering, and a plot showing the difference between the first two. A total of four days of data were accumulated with approximately ten runs being taken each day. Three distinct sources were used on different days, one source being used twice. The remaining three days' data were divided so there were about two runs with the resonant scatterer to each run with the non-resonant scatterer. The average result of all of these runs is the result which is reported here.

In order to obtain a correct idea of the differences between the data for the resonant case and the non-resonant case, one must somehow correct these data for the decrease in source activity in time and the dead time of the electronics. The first of these adjustments was done through the expression

$$N = N_o e^{-\lambda t}$$

which describes the exponential decay of the quantity N whose initial value was N_o, with λ being the decay constant and t being time. Integration of this expression over a time inverval Δt beginning at t_1 shows that the average value of N in the interval Δt, $\bar{N}$, may be used to find the initial value, N_o, provided λ and t_1 are also known. For this purpose

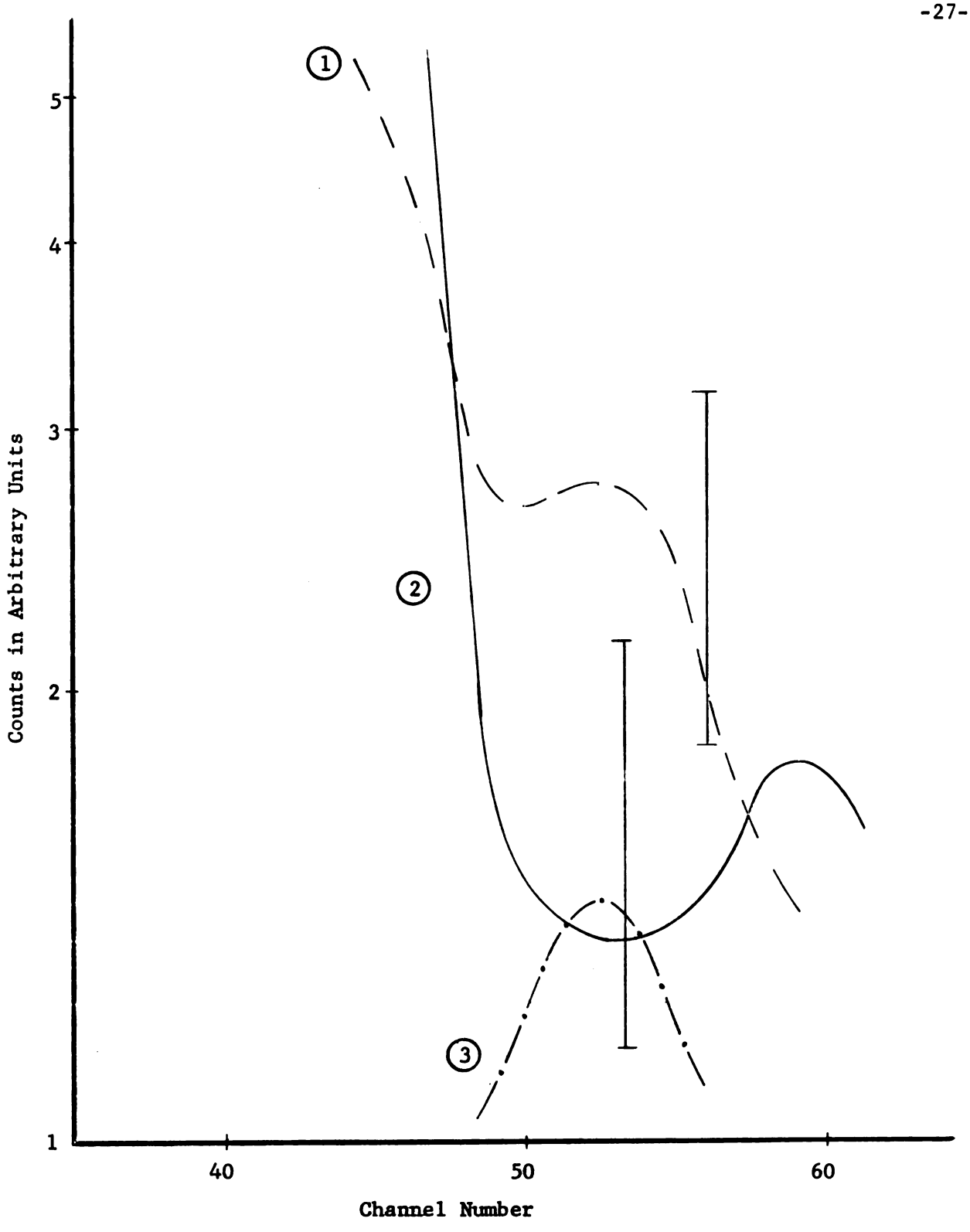

COMPOSITE PLOT OF ONE DAY'S DATA

(1) Resonant Scatterer — — — (2) Nonresonant Scatterer ———

(3) Difference — · —

FIGURE 10

$$N_o = \frac{\bar{N}\,\lambda\Delta t}{1 - e^{-\lambda\Delta t}}\, e^{\lambda t_1} \qquad (1)$$

For the present case of the 54-minute activity of Sn^{116}, which gives rise to the 1.27 Mev level, the decay constant is found to be

$$\lambda = 0.0128 \text{ min}^{-1}.$$

This value for λ was used in equation (1) to correct the data for source decay.

The second adjustment of the data, that for the dead time of the electronics, is an integral part of the design of the R.I.D.L. 256 channel pulse height analyzer used in the measurements. This correction caused the counting periods to be somewhat longer than the time during which the measurements were actually being taken. For example, if a dead time of 25% were maintained throughout a counting period of length T, the actual length of time during which counting was being done would be 0.75T. This corrected length of counting period must be used in place of Δt in equation (1) to account for dead time. Such corrections were made in all cases.

Further calibrations are required, as mentioned in Section II, to allow for the various parameters of the experiment other than the cross-section for resonant scattering. Thus, equation (4) of Section III must be modified to take into account these parameters.

The number of gamma-rays impinging on the scattering ring, $N'(E_\gamma)$, is given by

$$N'(E_\gamma) = N\Omega_s,$$

where Ω_s = fractional solid angle subtended by the scattering ring at the source.

Also, the number of resonantly-scattered gamma-rays detected by the crystal, S, is related to the total number of resonantly-scattered gamma-rays, S', through the expression

$$S = S' \Omega_D A \eta p d,$$

where D = fractional solid angle subtended by the crystal at the scattering ring,

A = absorption by the graded Sn-Pb absorber,

η = efficiency [16] of the crystal,

p = photofraction,

and d = non-selective electronic absorption in the ring obtained from the average value of $e^{-\mu_1 x}$ over the depth of the scatterer, where $\mu_1 = 0.0484$ cm^2/gm, and x = scatterer depth in gm/cm^2. In this case, $d \simeq 0.81$.

The factors Ω, A, η, and p are determined as a single factor f taken from the mean value of the plot in Figure 6.

Hence, the expression which may be used to calculate the average cross-section for resonance fluorescence from the scattering data is

$$S = N \Omega_S \Omega_D \sigma_{av} A \eta p n q \qquad (3)$$

where q = term representing the selective absorption by the scatterer. For this case $q \simeq 1$ since the scatterer is essentially thin [10],

n = number of Sn^{116} nuclei per cm^2 in the scatterer.

This expression may now be used in conjunction with equation (4) of Section III to find the lifetime of the 1.27 Mev state.

In all cases the source strength was of the order of one millicurie (with the exception of the first day's set of runs which were not used due to the very weak source) under the 1.27 Mev peak. The number of counts registered which could be attributed to resonantly-scattered radiation was extremely low; in fact, it was of the order of magnitude of the statistical error. The result obtained for the lower limit average cross-section was $1.3 \pm 1 \times 10^{-2}$ barns. With this value for σ_{av} the value for the upper limit of τ from equation (5), Section III, becomes $0.84 \pm .7 \times 10^{-12}$ seconds.

Conclusions

The result that τ is less than 0.84×10^{-12} seconds differs by a factor of two from those results quoted in [14] and [15]. Coulomb excitation in [14] yielded a lifetime of 0.5×10^{-12} seconds, while resonance fluorescence [15] gave a value of 0.33×10^{-12} seconds for τ. The very low counting rate, of the order of one count per second, which could be attributed to the resonant peak, contributed to the large statistical errors in the present result.

It has been suggested [16] that the weakness of the source, coupled with the small cross-section and a high background of non-resonant scattered counts, helped to obscure the resonance peak. Because of this it was not possible to accumulate the large number of counts necessary to measure the effect accurately. Reference [15] has shown that experiments with more active sources give better results.

BIBLIOGRAPHY

1. W. Kuhn, Phil. Mag. 8, 625 (1929)
2. F. R. Metzger, Phys. Rev. 83, 842 (1951)
3. F. R. Metzger and W. B. Todd, Phys. Rev. 91, 1286 (1953)
4. P. B. Moon, Proc. Phys. Soc. Lond. A64, 76 (1951)
5. K. G. Malmfors, Arkiv Fysik 6, 49 (1952)
6. F. R. Metzger, Phys. Rev. 103, 983 (1956)
7. N. Delyagin, Sov. Phys. JETP 37(10), 837 (1960)
8. Handbook of Physics and Chemistry, 37th edition, C. D. Hodgman, ed. (Chemical Rubber Publishing Co., Cleveland, Ohio)
9. F. R. Metzger, "Resonance Fluorescence in Nuclei" in Progress in Nuclear Physics, O. R. Frisch, ed., (Pergammon Press), pp. 59-60
10. M. E. Rose, Internal Conversion Coefficients, (Interscience Publishers, Inc., New York)
11. C. P. Swann and F. R. Metzger, Phys. Rev. 108, 982 (1957)
12. S. Ofer and A. Schwartzchild, Phys. Rev. 116, 725 (1959)
13. N. R. C. Data Sheets
14. G. B. Beard and W. H. Kelly, Nuc. Phys. 43, 523 (1963)
15. W. H. Kelly, Private Communication (1963)
16. F. R. Metzger, Phys. Rev. 101, 286 (1956)
17. Evans, R. D., The Atomic Nucleus (McGraw-Hill Book Co., New York) 1955, pp. 685-88